DISLOCATION IMAGING WITH BRAGG COHERENT X-RAY DIFFRACTION IMAGING UNDER POISSON NOISE

A Thesis
Presented to the Faculty of the Graduate School
Of Cornell University
In Partial Fulfillment of the Requirements for the Degree
of Master of Science

By
Yumeng Song
December 2024

ABSTRACT

Bragg Coherent Diffraction Imaging has been applied to nanomaterial characterization for imaging atomic movement and phase transformation. Its ability to produce unique three-dimensional defect and displacement field images has been extremely helpful for understanding material property under different environment, such as energy cells or optical materials in various working conditions. In this study, we use computer simulations to reveal the influence of Poisson noise on the resultant reconstruction images of atomic defects within a nanoparticle. The study focuses mainly on dislocation imaging, including dislocation loops. By simulating the reconstructions under different Poisson noise level, we defined the threshold of the Poisson Noise level for different number of dislocations in the atomic structure. We have also discovered the effects of the size and shape of the dislocation loops.

BIOGRAPHIC SKETCH

Yumeng Song received her bachelor's degree in material science at Cornell in 2022. She joined the Master Program in Materials Science and Engineering department at Cornell University in 2022 and has worked with Professor Andrej Singer on Bragg coherent diffraction imaging of energy materials since then.

ACKNOWLEDGEMENTS

First, I want to express my gratitude to my advisor Prof. Andrej Singer, who has offered great help and support during the past two years. He has introduced me to the field of X-ray and taught me how to conduct research independently since my undergraduate study. He has also provided me with great mental support.

I would also like to thank my committee Prof. Jin Suntivich. I am also grateful to my group members, especially Yifei Sun who has given me a lot of support on my research. I really learned a lot from each one of my group members through exchanging ideas and learning from their experiences.

Table of Contents

Introduction

1.1 Dislocations

A dislocation, by definition, is a linear crystallographic defect. When the atomic arrangement is distorted, where one plane is slightly off with another plane of atom, forming an extra-half plane, edge dislocation is present. The dislocation line is perpendicular to the Burger's vector for an edge dislocation case [1]. In comparison, when the Burger's vector is parallel to the dislocation line, it would be a screw dislocation. A screw dislocation, as shown by its name, forms a spiral motion dislocation line. The resulting atomic structure is like one half is slightly rotated to the direction of the dislocation propagation. [2]. An example of screw dislocation is shown in **Figure 1**.

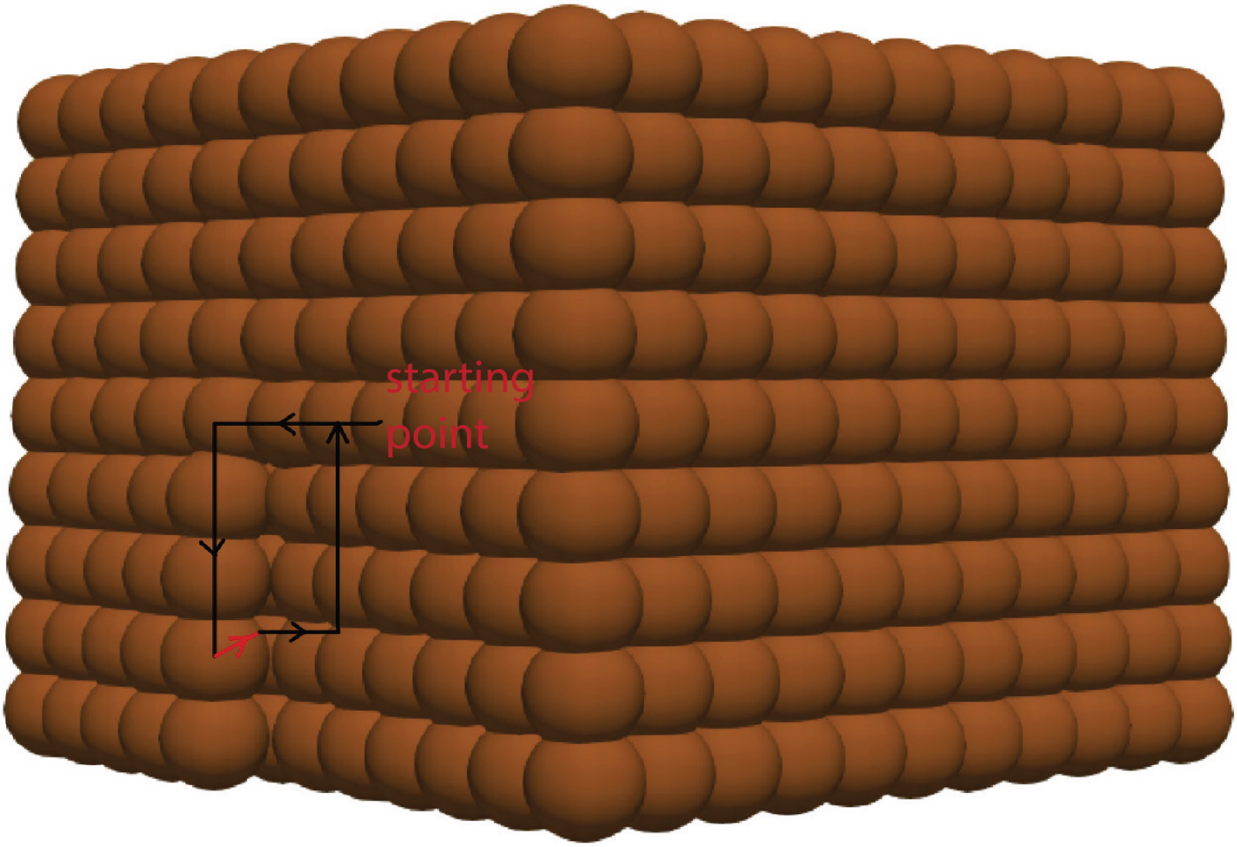

Figure 1. A three dimensional screw dislocation. The Burger's vector is marked in red.

The Burger's vector is very important when people need to obtain the magnitude and direction of the lattice distortion associated with a dislocation. It is represented by the closure failure of a loop around the dislocation line and is invariant for a given dislocation [3], as marked by the red arrow in **Figure 1**. The interaction between the Burger's vector and the dislocation line determines the type and behavior of the dislocation. We will see this later in this study.

Dislocations are not static but can move through the crystal lattice under the influence of external stresses. The movement of dislocations can significantly change the shape and size of a nanoparticle, which could further influence the properties of a nanoparticle. The ease of dislocation motion, or slip, depends on the crystal structure, temperature, and applied stress [4].

Dislocation motions and piling up may lead to fracture inside a material. This could result in plastic deformation. Therefore, materials with a high density of dislocations typically exhibit significant plasticity [5].

Dislocation interactions are another key aspect of dislocation theory. When dislocations intersect, they can annihilate, form jogs, or generate new dislocation segments. Sometimes there could be dislocation loops, formed by dislocation intersections at specific angles under different conditions. We have to mention dislocation density, which is the total length of dislocation per unit volume. It measures the number of dislocation inside a material [6]. When dislocation density increases, the material is work harden, and will become more resistant to more deformations [7].

1.2. Bragg Coherent Diffraction Imaging

Nowadays, modern material industry has developed to a new state, where nanomaterial and nanotechnology has emerged and changed the modern society. The discovery and application of nanomaterials was supported by X-ray diffraction (XRD). Because the wavelength of X-ray matches the size of crystalline materials, their characterization was finally possible. The characterizations of their crystal structure, phase identification, and other material properties have paved the way to their material application in various fields. Therefore, people have tried to improve XRD technique. As a result, Bragg Coherent Diffraction Imaging (BCDI) was discovered, and it shined a new light on nanoscale characterization [8].

One great advantage of XRD is its non-destructive nature. X-ray is a type of electromagnetic wave with a certain wavelength, and therefore it can penetrate through a

material sample without breaking its surface or interior. It can therefore give material structure and composition, by capturing its reflected X-Ray using a detector. The reflected X-ray is an electromagnetic wave that contains all the information of the sample. The constructive interference of the X-ray with the atoms would give certain diffraction patterns and images, which would be analyzed to yield the structure and composition information[9]. Bragg's Law is the fundamental principle behind XRD, which states that when the path difference between the reflected rays is an integer multiple of the incident wavelength:

$$n\lambda = 2dsin(\theta)$$

there would be constructive interreferences.

An XRD experiment typically consists of rotating the sample or the detector. Rotating the sample is called a rocking scan and is usually used to measure crystal quality. A two-theta scan is when the sample and the detector are both rotated and is mainly used to measure lattice constants and strain information. A diffraction pattern would be recorded by the detector, which could be a point detector or a line detector [10]. XRD technique are applied in many fields for different types of materials, including metallurgy, ceramics, polymers, pharmaceuticals, and geology [11].

Nanoscale detection of strains and defects requires more precise and accurate measurements. The traditional XRD failed to detect defects, such as dislocations or grain boundaries. In comparison, Bragg Coherent Diffraction Imaging (BCDI) resolves these issues by combining coherent X-ray diffraction with phase retrieval algorithms. The resulting images are three dimensional, which the conventional XRD can only yields 2D images. The defect fields and displacements field can also be detected with high resolution [12].

BCDI differs from regular XRD in several key aspects. Unlike traditional XRD, which measures the intensity of scattered X-rays, BCDI exploits the coherence of synchrotron X-ray

sources to capture the phase information of the diffracted waves. This is achieved by illuminating a single crystalline domain with a coherent X-ray beam and measuring the resulting diffraction pattern around a Bragg peak. The recorded diffraction pattern is then subjected to iterative phase retrieval algorithms to reconstruct the real-space electron density and phase distribution within the crystal [13].

The discovery and development of BCDI can be traced back to advancements in X-ray sources and detectors, as well as computational techniques for phase retrieval. The technique was pioneered in the early 2000s, with significant contributions from researchers working at synchrotron facilities. Key developments included the ability to produce highly coherent X-rays and the implementation of algorithms capable of reconstructing three-dimensional images from coherent diffraction data [14].

1.3 Reconstruction

Reconstruction is a crucial process in Bragg Coherent Diffraction Imaging (BCDI) that involves converting diffraction data into real-space images of a crystal's internal structure. The term "reconstruction" refers to the method of retrieving the electron density and phase information of a crystal from its diffraction patterns. This process is crucial for visualizing the distribution of defects, strains, and other nanoscale features within the material, providing detailed insights that are not accessible through traditional imaging techniques.

One of the fundamental challenges in diffraction techniques, including BCDI, is the phase problem. When X-rays are diffracted by a crystal, detectors record only the intensity of the

diffracted waves, losing the phase information. This loss of phase information prevents a straightforward reconstruction of the crystal structure from the measured diffraction pattern. The phase problem is significant because the phase contains crucial information about the relative positions of atoms within the crystal. Without phase information, it is impossible to accurately reconstruct the real-space image of the crystal. Solving the phase problem is, therefore, essential for obtaining meaningful and accurate reconstructions in BCDI [15].

The process of phase retrieval is an iterative computational method used to recover the lost phase information from the measured diffraction intensities. This method involves alternating between real space and reciprocal space, applying constraints in each domain to progressively refine the phase estimation. **Figure 2** illustrates this iterative process, where F denotes the Fourier transform and F^{-1} denotes the inverse Fourier transform.

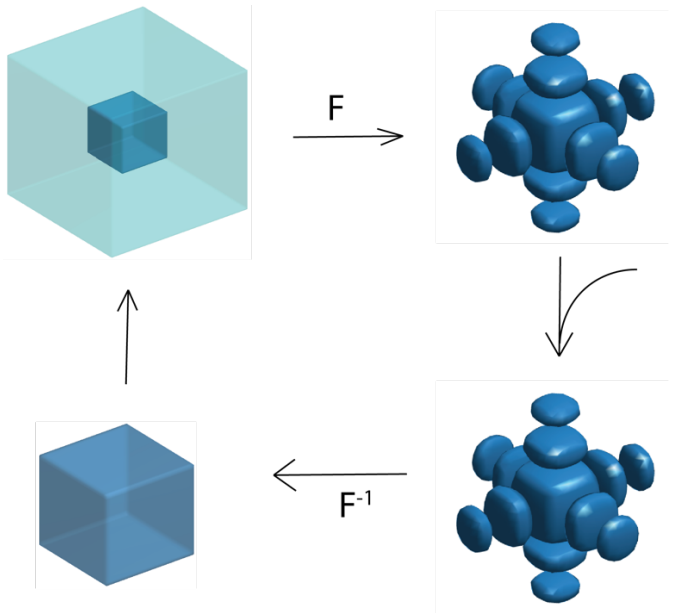

Figure 2. The Phase retrieval algorithm. A real value constrain is put on the particle matrix, then the matrix with the constrain goes through a Fourier transform to get the diffraction pattern. The inverse Fourier transform gives back the information of the particle.

The detailed procedure of phase retrieval, often referred to as the phase loop, includes the several steps. The phase retrieval algorithm illustrated is an iterative process, and each loop is shown by the arrows. The first step is to basically guess a phase and assign it to the measured intensity data. This guess is done by taking the Fourier transform of the real space intensity data, and the result is the reciprocal space in the up right conner. Then we inversely Fourier transform the reciprocal space data with the guessed phase data back to real space, and the result would be some random real space particle. The next step is to create a real space constrain outside the particle, which is represented by the transparent box outside the particle. This physical and chemical constrain on the electron density map makes the guessed particle more realistic. Then the resulting particle and the real space constrain together are Fourier transformed to the reciprocal space, so we are back to the upper right corner of the loop now. The process is repeated until the particle in real space is the actual particle, and the phase information that has the strain and defect fields in it is now successfully retrieved.

The phase retrieval process is essential for obtaining high-resolution, three-dimensional images of the crystal's internal structure, allowing researchers to visualize and analyze nanoscale defects and strain distributions with unprecedented detail [16].

1.4 Poisson Noise

In the context of Bragg Coherent Diffraction Imaging (BCDI), Poisson noise is an inherent source of uncertainty that arises during the detection of X-ray photons. Understanding the nature and implications of Poisson noise is crucial for accurate image reconstruction and interpretation of the results.

The presence of Poisson noise is due to the discrete nature of photon. In quantum mechanics, photons are quantized, meaning that they can only take on integer numbers. When

the reflected X-rays reaches a detector, individual photons are counted over a specified time interval. The detector must count the photons as integer numbers. So when the photon number is significantly low, such as 0.01 photon, the detector has to count it as 0 or 1 photon. The choosing between 0 and 1 follows a Poisson process. In this case, it would describe the probability of the detector counting a low number of photon as 0 or as 1 photon.

The Poisson nature of photon counting leads to inherent variability in the number of detected photons, even under identical conditions. This variability manifests as Poisson noise, which impacts the signal-to-noise ratio (SNR) and the precision of the measured diffraction patterns.

In practical terms, Poisson noise introduces fluctuations in the intensity measurements recorded by the detector. These fluctuations are particularly significant in regions of low photon count, where the relative uncertainty is higher. As the number of detected photons increases, the relative impact of Poisson noise decreases, improving the SNR and the reliability of the measurements [17]. Understanding Poisson noise is critical for accurate phase retrieval and image reconstruction in BCDI.

METHOD

To understand the effect of Poisson noise on reconstruction, a simulation of particles was created. In this simulation, a simple shape particle, a cube with one edge cut, is created. In this cubic particle, a dislocation is created using the following equation

(1) $$ux = \tan^{-1}(x, y)$$

Then the diffraction pattern of this defective particle was calculated. In a real experiment that undergoes BCDI, the diffraction pattern is captured by the detector. Here, we used a series of computer algorithms to calculate the diffraction pattern.

The scattering amplitude A(q)and the diffraction intensity I(q)are related to each other as shown in equation 2

(2) $$I(q) = A(q)^2$$

Where q denotes the momentum transfer vector and $q = kf - ki$ is the difference between the scattered and incident wave vectors. So to calculate the intensity pattern, the scattering amplitude must be known. In general, the scattering amplitude A(q)is obtained by taking the Fourier transform of a complex function,

(3) $$S(r) = s(r)exp(-i\varphi(r))$$

r is a point in the reciprocal space. This complex function is composed of an amplitude function s(r)and a complex exponential function containing the phase function $\varphi(r)$.

In this experiment, S(r)became

(4) $$S(r) = cube \cdot exp(i \cdot ux)$$

The amplitude function is the function of the cubic particle, denoted as cube, and (r) is replaced by the dislocation function, which is consistent with the convention that the defect information is always included in the phase function. Now, taking the Fourier transform of this S(r) yielded the scattering amplitude A(q), and the diffraction intensity and the diffraction pattern can then be calculated.

After calculating the diffraction pattern, Poisson noise is inputted using equation 5.

(5) $$I(q) = Poisson(I(q)/(I(q)_{sum} \cdot \#photon))$$

After normalizing I(q)with the product of the maximum intensity and the number of photons, I(q)underwent a Poisson process. When the incident beam is scattered by the sample particle, the detector captures the scattered beam and counts the number of photons. The counting process undergoes a Poisson process when the number of photons is not an integer number. Therefore, in the calculation, the influence of Poisson noise is calculated using a Poisson process. The level of

noise was increased throughout the experiment by altering the number of photons. Finally, the diffraction pattern along with the Poisson noise is put under reconstruction.

RESULT AND DISCUSSION

The following section presents the results of our study on the impact of varying separation distances between two screw dislocations on the resulting X-ray diffraction patterns. This analysis is critical for understanding the sensitivity of Bragg Coherent Diffraction Imaging to dislocations in crystalline materials.

3.1 Two Dislocation Separation

As a baseline comparison, Figure 3 presents the diffraction image of a particle with no dislocation, depicting a pure particle without defects. This image serves as a reference for assessing the impact of dislocations on the diffraction patterns.

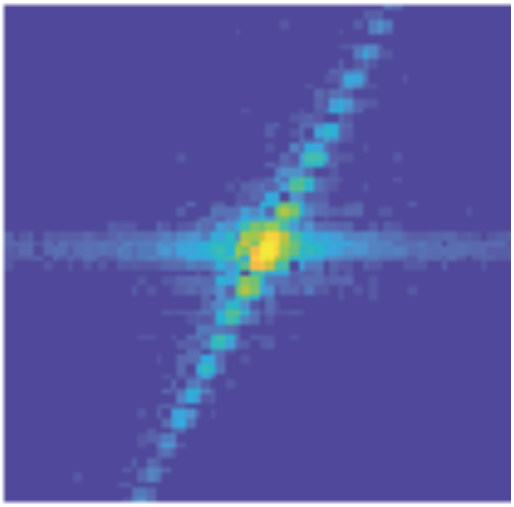

Figure 3. A diffraction pattern of a perfect particle without defect. A complete peak is at the center.

The impact of varying separation distances between two screw dislocations on the resulting X-ray diffraction (XRD) patterns are shown in **Figure 4**. During screw dislocation propagation, there are two scenarios: the direction of propagation is in the same direction as the Burger's vector, or the direction of propagation is in the opposite direction as the Burger's vector. Here we demonstrate how the separation between 2 screw dislocations changes the diffraction image.

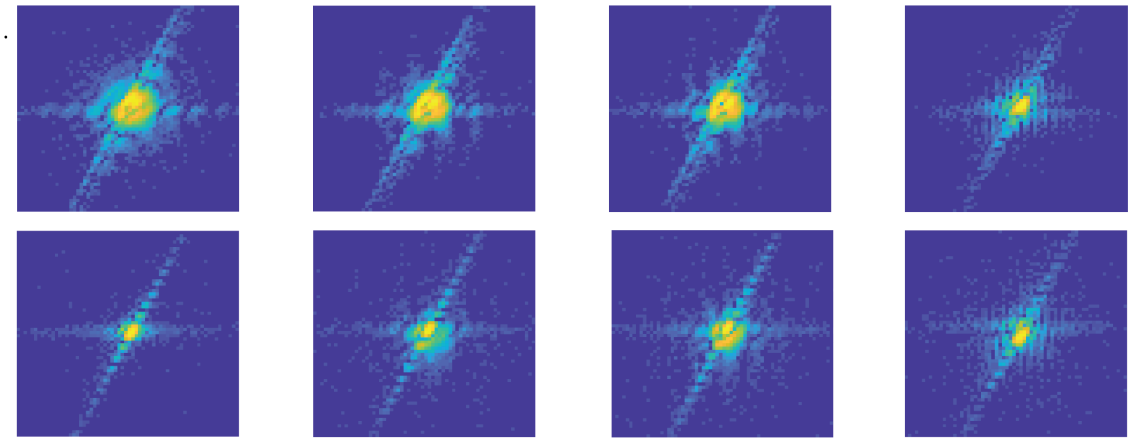

Figure 4. Diffraction pattern with two dislocations moving out with the same direction Burger's vector (first line), and with two dislocations with opposite direction Burger's vector (second line).

The position and separation of the dislocations in real space are illustrated in **Figure 5**.

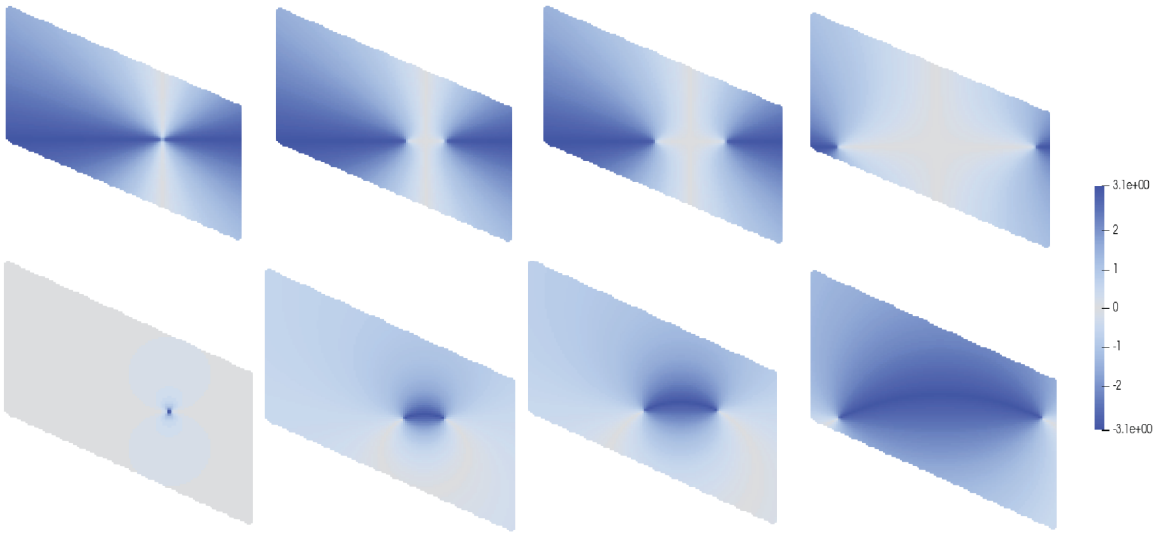

Figure 5. Real space (Input) of the phase. The first line shows when the 2 screw dislocations has the same Burger's vector, and the second line is when they have opposite direction Burger's vector.

Clearly, XRD is very sensitive to 2 dislocations with same direction Burger's vector, because even when the separation is very small shown by the first images in the figure, the diffraction image can still capture the peak broadening and separation. The peak broadening is very obvious compared with the no dislocation image in **Figure 3**. As the separation increases from the left to the right, also shown by the images in **Figure 5**, the two singularities in the yellow diffraction peaks becomes increasingly clear to see. However, when the separation becomes too large, shown by the last image in the series, XRD loses the sensitivity to dislocations, and the diffraction image looks identical to the no dislocation case.

When the 2 Burger's vectors are in opposite directions, it becomes harder for XRD to capture the dislocations in the diffraction images. As shown in **Figure 5**, when the 2 dislocations are very close to each other, the diffraction image also looks identical to the no dislocation case. This is because the 2 opposite direction Burger's vector makes the 2 dislocations annihilate each other when they are very close to each other. This annihilation resulted in no dislocation detected in the diffraction pattern. As the separation increases, the diffraction peak changes and the atomic distortion are shown by the shift of intensity in the diffraction peak. When the separation gets extremely high, the diffraction pattern gets back to be a no dislocation case, and this is the same case with the 2 same direction Burger's vector case.

Overall, BCDI is more sensitive to 2 screw dislocation with the same direction Burger's vectors, which BCDI could show the existence of defect in the diffraction pattern even when the 2 dislocations are very close to each other. Whereas when they have 2 very close dislocations with opposite direction Burger's vectors, diffraction image alone cannot correctly indicate whether or not there are defects in the atomic structure. A more detailed check with reconstruction is necessary. This is also true for the extremely high separation condition for both Burger's vector cases.

3.2 Reconstruction Threshold

In this study we have found that to obtain a successful average reconstruction with the clear phase information, only 50% of the single reconstructions needs to be successful, as shown in **Figure 6**. The graph shows the relationship between a phase wrap and the corresponding successful number of reconstructions. After the number exceeds 5 out of 10 reconstructions, the phase wrap has stayed at 2π, which is a singularity in the phase that indicates a dislocation in the real space. This is way fewer than our initial guess that around 70% of the single reconstructions

need to be successful for the average reconstruction clearly showing the phase wrap. This also means even when the average reconstruction fails, one can still dive into the single reconstructions for clues of dislocations. For example, if 40% of the single reconstructions show the dislocations and they looks similar to each other, meaning they are not randomly given by the iterative process of reconstructions, then one can still conclude the existence of a dislocation in the particle.

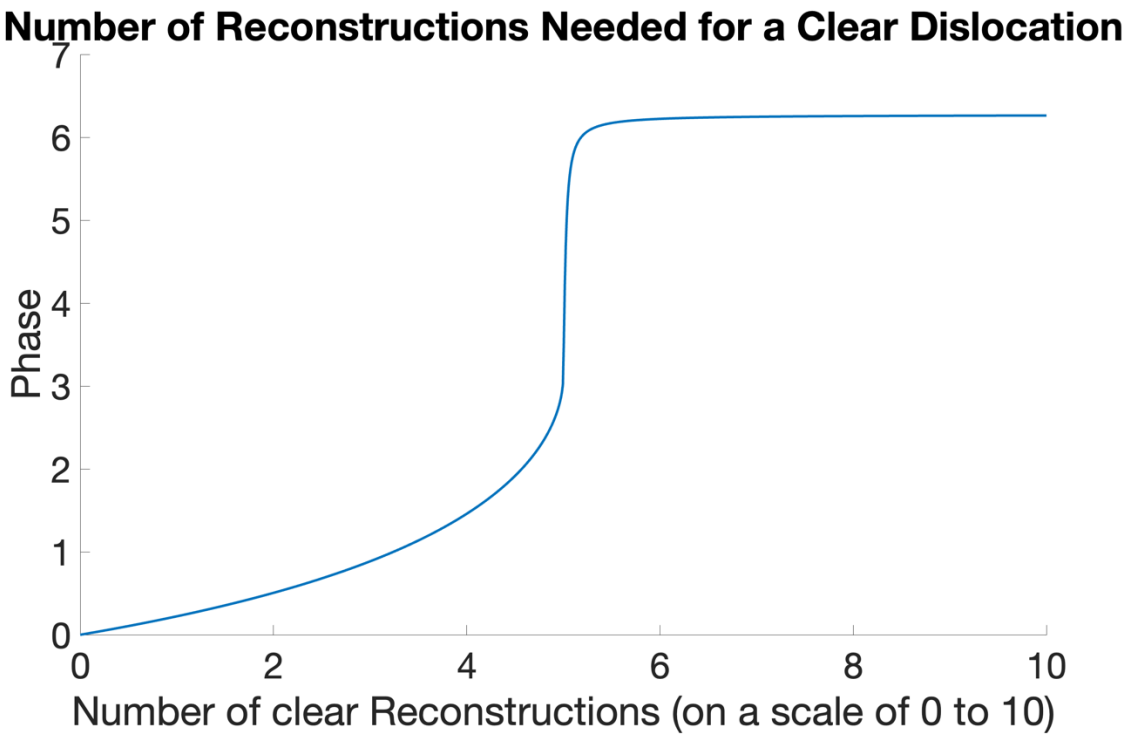

Figure 6. A graph showing the necessary number of clear reconstruction for a successful average reconstruction. It shows that 50% single reconstructions are essential.

In conclusion, to obtain a reconstruction that clearly shows a dislocation, at least 50% of the single reconstructions need to be successful. This provides an alternative method of analyzing dislocation existence in a particle, which is when the average reconstruction does not work, the single reconstructions could be useful.

3.3 Dislocation Loop

The threshold is supported by **Figure 7**. Here we demonstrate dislocation loops, which is a more realistic case. The average reconstruction fails when photon number is 100, which is a very high level of Poisson noise. However, if we look at the average reconstruction, we could see some of them still shows a similar phase arrangement that indicates the presence of a dislocation loop. However, since the number is less than 5 out of the 10 single reconstructions, the average reconstruction does not show the same phase arrangement for the dislocation loop.

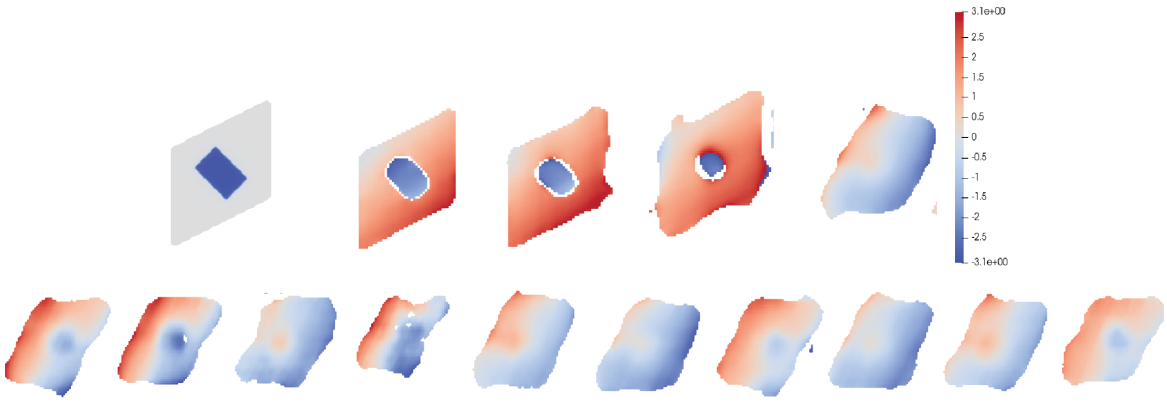

Figure 7. A cubic particle with a dislocation loop inside. The average reconstruction with total photon number of 1000000, 100000, 10000, 1000. With 1000000 photons, a clear loop of singularity is visible. The loop eventually disappear when photon drops to 1000.

We have also discovered the influence of the size and shape of the dislocation loops on the reconstruction quality. As shown in **Figure 8**, which demonstrates that a square dislocation loop is easier to reconstruct than a rectangular loop, and the larger the loop the easier the reconstruction. The first line is the 2D slices cutting through the x-y plane, and the second line is cutting through the x-z plane. The graph shows the change in phase around the singularity point cutting through the x-z plane. At 100 photon level, the phase shift captured by reconstruction for the rectangular loop is less than that of a square loop, proving that square loops are easier to

reconstruct. The third line is also a square, but with a smaller size, which is almost like a circle. The size of the loop plays a very crucial role. The reconstruction completely failed at 100 photon level.

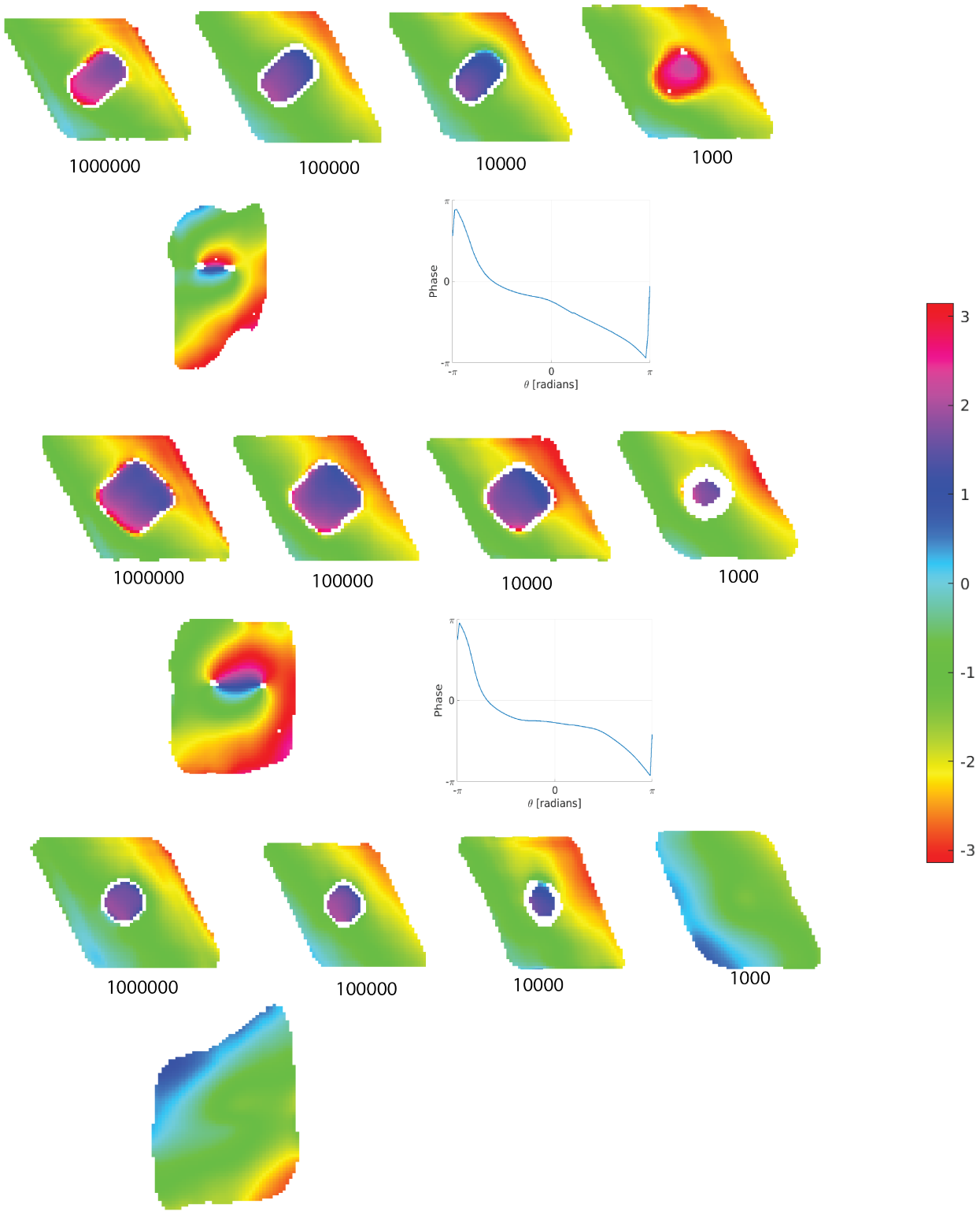

Figure 8. Showing the impact of the size and shape of the loop on reconstruction quality. A larger loop is easier to reconstruct, requiring less photon.

CONCLUSION

In this study, we have extensively explored the capabilities and limitations of Bragg Coherent Diffraction Imaging (BCDI) for dislocation imaging within nanoparticles, particularly focusing on the influence of Poisson noise on reconstruction quality. Through a series of computer simulations, we investigated the sensitivity of X-ray diffraction (XRD) and BCDI to various configurations of screw dislocations, analyzing both the effects of dislocation separation distances and Burger's vector orientations.

Our findings indicate that BCDI is particularly sensitive at detecting screw dislocations with the same direction Burgers vectors, even at small separations, which is evident through the clear peak broadening and separation in diffraction patterns. Conversely, dislocations with opposite direction Burgers vectors are more challenging to detect due to the potential for dislocation annihilation, which often resulted in diffraction patterns resembling those of defect-free particles.

Moreover, we established that to achieve a successful average reconstruction with clear phase information, at least 50% of the single reconstructions must be accurate. This threshold provides a practical benchmark for assessing reconstruction success and underscores the potential of individual reconstructions to reveal dislocation presence, even when average reconstructions fail.

In examining dislocation loops, we observed that the size and shape of the loops significantly impact reconstruction quality. Larger, square-shaped loops were easier to reconstruct, requiring fewer photons to achieve clear phase shifts, compared to smaller or rectangular loops.

Overall, our study demonstrates the robust capabilities of BCDI in visualizing nanoscale defects and strains within crystalline materials. The insights gained from this research enhance our understanding of material properties under different environmental conditions and provide a foundation for future advancements in nanoscale imaging and materials characterization.

REFERENCES

1. Hull, D., & Bacon, D. J. (2011). Introduction to Dislocations. Butterworth-Heinemann.
2. Hirth, J. P., & Lothe, J. (1982). Theory of Dislocations. John Wiley & Sons.
3. Anderson, P. M., Hirth, J. P., & Lothe, J. (2017). Theory of Dislocations. Cambridge University Press.
4. Nabarro, F. R. N. (1967). Theory of Crystal Dislocations. Dover Publications.
5. Courtney, T. H. (2000). Mechanical Behavior of Materials. McGraw-Hill.
6. Li, J. C. M. (1969). Dislocation Density and Stress Strain Relations in Polycrystals. Transactions of the Metallurgical Society of AIME, 245, 1249-1254.
7. Meyers, M. A., & Chawla, K. K. (2009). Mechanical Behavior of Materials. Cambridge University Press.
8. Gorobtsov, O., & Singer, A. (2022). Shear displacement gradient in X-ray Bragg coherent diffractive imaging. *Journal of Synchrotron Radiation*, 29, 866-870.
9. Gao, Y., Huang, X., Harder, R., Cha, W., Williams, G. J., & Yan, H. (2022). Modeling and experimental validation of dynamical effects in Bragg coherent x-ray diffractive imaging of finite crystals. *Physical Review B*, 106(18), 184111.
10. Cullity, B. D., & Stock, S. R. (2001). Elements of X-ray Diffraction. Prentice Hall.
11. Jenkins, R., & Snyder, R. L. (1996). Introduction to X-ray Powder Diffractometry. John Wiley & Sons.
12. Robinson, I. K., & Harder, R. (2009). Coherent X-ray Diffraction Imaging of Strain at the Nanoscale. Nature Materials, 8(4), 291-298.
13. Ulvestad, A., & Yau, A. (2017). Bragg Coherent Diffraction Imaging of Single-Particle Dynamics. Annual Review of Physical Chemistry, 68, 229-251.

14. Hofmann, F., Phillips, N. W., Das, S., Daranciang, D., Ernst, F., Harder, R. J., Holt, M. V., & Clark, J. N. (2018). Nanoscale Imaging of Strain Evolution in an Individual Nanocrystal During Phase Transitions. Nature Communications, 9(1), 1-8.
15. Cha, W., Ulvestad, A., Harder, R., & Robinson, I. K. (2016). Imaging of Defect Dynamics in Nanoscale Particles by Coherent X-ray Diffraction. Nature Materials, 15(6), 690-695.
16. Miao, J., Charalambous, P., Kirz, J., & Sayre, D. (1999). Extending the Methodology of X-ray Crystallography to Allow Imaging of Micrometer-sized Non-crystalline Specimens. Nature, 400(6742), 342-344.
17. Pfeiffer, F. (2018). X-ray Ptychography. Nature Photonics, 12(1), 9-17.